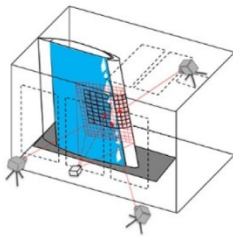


# Icing Wind Tunnel Test – Development of Real-time Ice Height Optical Measurement Method –



SATOSHI YONEMOTO\*<sup>1</sup> SUGURU HASE\*<sup>2</sup>

YOICHI UEFUJI\*<sup>3</sup> GENTO ICHIKAWA\*<sup>4</sup>

HIROYUKI TANAKA\*<sup>5</sup>

*A wing anti-ice system for commercial aircraft that considers environmental impact and aircraft fuel efficiency should be designed to consider both the degradation of engine performance and the appropriate evaluation of ice accumulation on the area behind the protected surface of the wing, referred to as “runback ice”.*

*Generally, the ice shape is evaluated by icing wind tunnel testing. However, since ice has the characteristics of shedding and accumulating processes, it is impracticable for the ice shape to be directly captured and measured because the ice tends to break off and vary due to the fluctuating wind when the wind tunnel shuts off. This report introduces a new optical measurement system that Mitsubishi Heavy Industries, Ltd. (MHI) has developed as a certifiable method for commercial aircraft.*

## 1. Introduction

When aircraft fly in icing conditions, referred to as visible moisture such as clouds and mist which contain supercooled water droplets, icing<sup>(1)</sup> occurs on an aircraft's lifting surfaces such as the main wing, tailplane, etc. and results in increases of wing/tailplane stall speed (or decrease of stall angle) and drag, which may affect the aircraft's stability, controllability and performance<sup>(1)(2)</sup>. Hence, there are regulations to show compliance with the requirement that commercial aircraft can safely fly in icing conditions<sup>(3)(4)(5)</sup>. In order to show compliance with these regulations, it is common for commercial aircraft to install a wing anti-ice system using high temperature bleed air supplied from the aircraft engines<sup>(1)</sup>. From an aircraft safety perspective, the installed wing anti-ice system should be verified in steps in order to evaluate its system performance corresponding to the simulation levels in development phases such as icing wind tunnel testing using a partial test model and natural icing flight testing using a full-representative aircraft. On the other hand, since the possibility of encountering the most severe icing condition is extremely low, the conventional practice in the industry is to perform the most severe performance testing in the assumed conditions by icing wind tunnel tests<sup>(6)</sup>.

The wing anti-ice system for lower surfaces of the wingspan, which considers environmental impact and aircraft fuel efficiency, is conventionally designed as a “running wet system” that only applies a limited amount of heat to prevent ice accumulation on the surfaces themselves, not to fully evaporate the water droplets that hit the surfaces.

In the design process, the appropriate evaluation of ice accumulation on the area behind protected surface during the system activates, referred to as “runback ice” is also required. Since runback ice has the characteristics of shedding and accumulating processes, there is the issue that it is impracticable that the ice size immediately before ice shedding is captured and directly measured by conventional methods<sup>(7)(8)</sup> after the tunnel stop because the ice tends to break off and vary due to the fluctuating wind when the wind tunnel shuts off. Thus, in the estimation of the effects on runback ice on flight safety, the ice shape must be overestimated by an additional margin considering the possibility that ice has grown from its true size immediately before shedding. In

\*1 Fluid Dynamics Research Department, Research & Innovation Center

\*2 Chief Staff Manager, Business Intelligence & Innovation Department, Technology Strategy Office

\*3 Chief Staff Researcher, Heat Transfer Research Department, Research & Innovation Center

\*3 Heat Transfer Research Department, Research & Innovation Center

\*1 Chief Staff Researcher, Fluid Dynamics Research Department, Research & Innovation Center

order to resolve this issue, this report presents the optical measurement system newly developed by MHI as a certifiable method for commercial aircraft.

## 2. Icing Wind Tunnel for Wing Anti-Ice System Performance

An icing wind tunnel test was carried out at NASA Glenn Research Center Icing Research Tunnel as a part of development tests for Mitsubishi SpaceJet. **Figure 1** gives an overview of the Icing Research Tunnel at NASA Glenn Research Center in Ohio, USA<sup>(9)</sup>. In the icing wind tunnel, the icing spray system was installed in front of the test section and icing conditions during actual flights were simulated on the ground by spraying the model with various supercooled water droplets characterized by median volume diameter (MVD) and liquid water content (LWC).

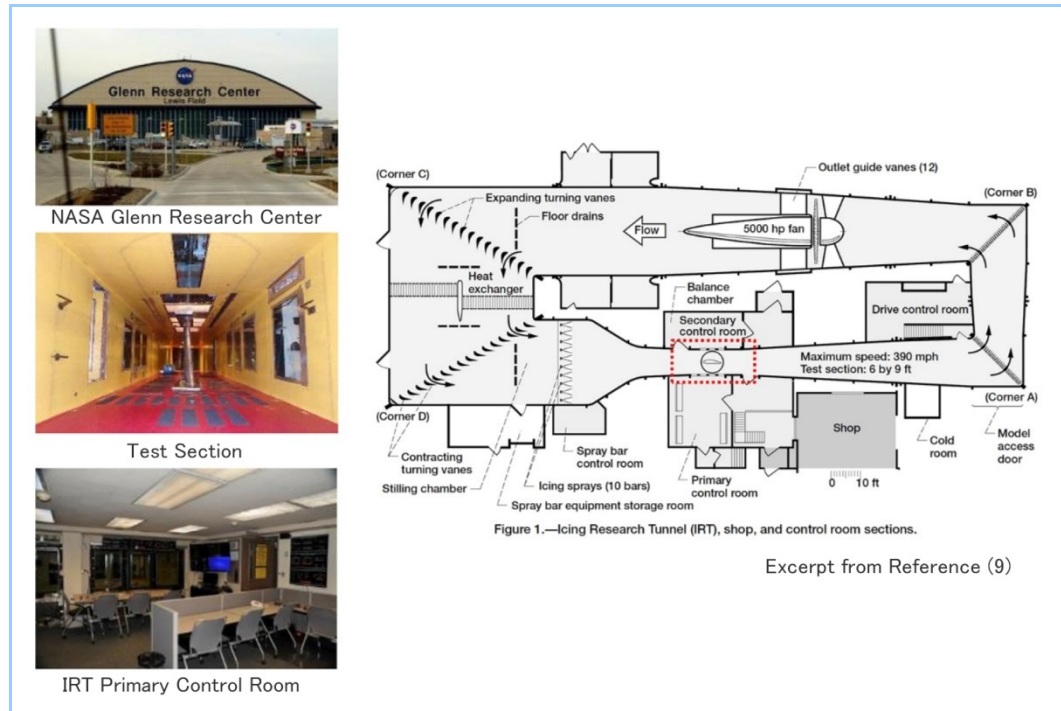


**Figure 1 Overview of NASA Glenn Icing Research Tunnel, Ohio, USA<sup>(9)</sup>**

**Figure 2** presents the schematic specifications of the icing wind tunnel test model and the test setup. The model was a right-hand-side full-scale partial model<sup>(10)</sup> that was designed with the limitation of wind tunnel blockage in mind and was produced by cutting out the outboard section of the main wing, where the anti-icing system is installed. The leading-edge high lift device (slat) was equipped with a piccolo tube to supply simulated high temperature bleed air and it had a function to thermally protect the slat by blowing the simulated hot bleed air into the inner surface of the skin. In the test, the image data of ice accretions on the model was acquired and slat temperature and pressure data were measured by the sensors in the model under the various conditions of the model configurations (high lift device is deployed/extracted, model angle of attack(AoA) and flow rate of high temperature bleed air) and wind tunnel settings (flow velocity, wind tunnel static temperature/total temperature and supercooled water specifications (LWC, MVD)).

**Figure 3** is an example of the images of a test to obtain runback ice on the lower surface of the wing. The test images reveal that the runback ice that accumulates in the rear of the slat anti-ice equipment grows corresponding to the spray time and the ice has the features of continuously and periodically shedding and accumulating.

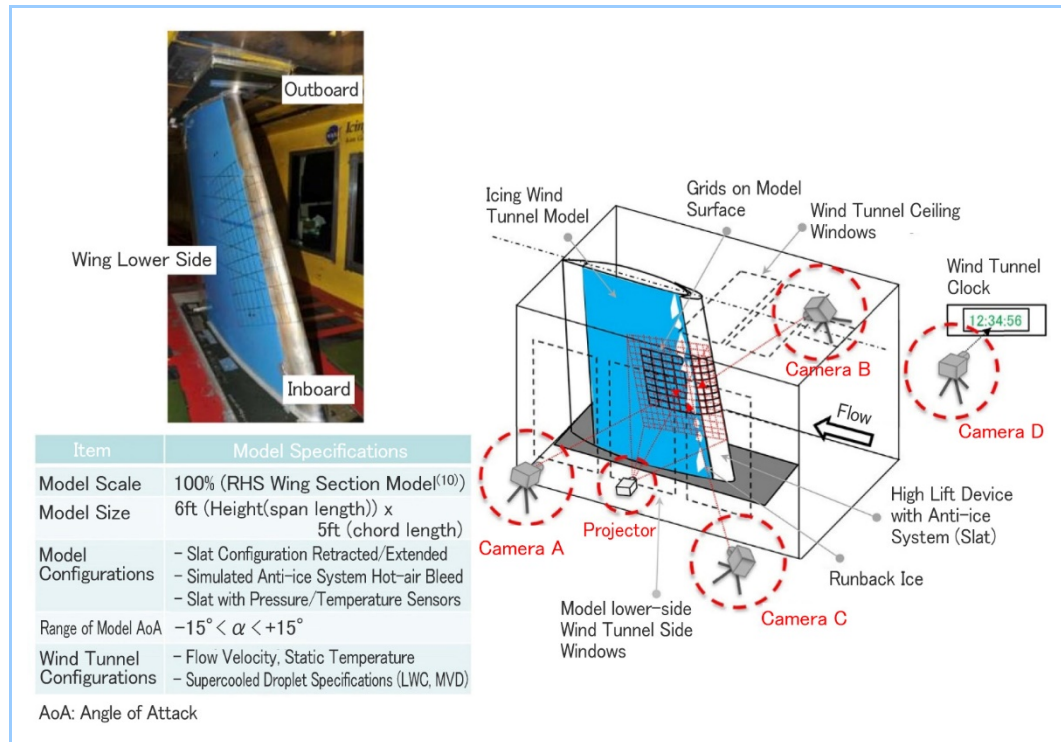


**Figure 2 Overview specifications of icing wind tunnel model and test setup**

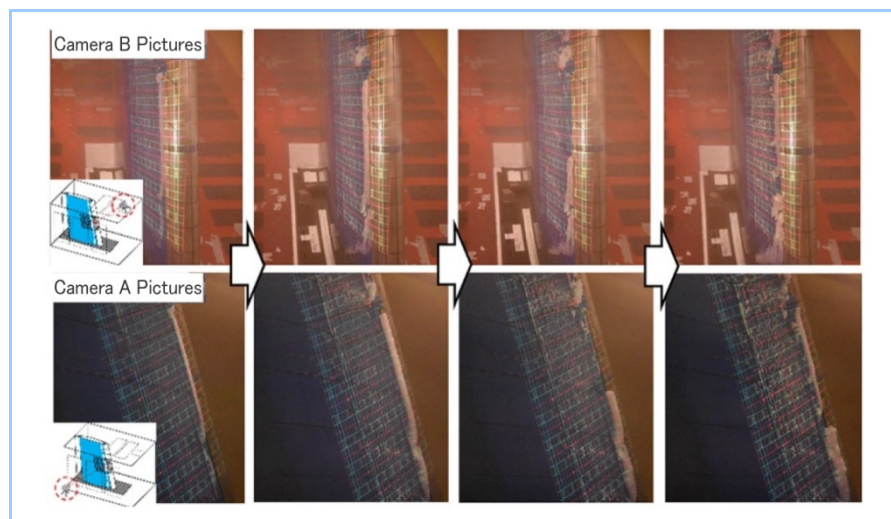


**Figure 3 Examples of acquisition test for wing lower-side runback Ice**

### 3. Optical Ice Height Measurement

In an icing wind tunnel test, it is common that after the wind tunnel is stopped, the accumulated ice on the model is cut by a preheated metal plate and its shape is directly traced on cardboard by hand as cross-sectional hand tracing method<sup>(7)</sup>, or the ice shape is scanned by three-dimensional laser equipment<sup>(8)</sup>. However, as the aforementioned characteristics of the runback ice targeted for this report, the conventional methods with sequential interruptions of the wind tunnel cannot capture and measure the actual ice size immediately before ice shedding because the ice tends to shed and alter owing to the fluctuating wind. On the other hand, the newly proposed optical measurement method provides a solution to acquire information such as the height, position and shape of ever-changing runback ice with applicable accuracy during testing. The details are described below.

#### 3.1 Test Setup for Optical Measurement

Figure 2 presents the test setup. Four still cameras (D 7200 (Nikon Corp.)) were installed at three locations where the model installed in the wind tunnel test section can be viewed stereoscopically from the ceiling, model rear and side windows. The other camera focused on the built-in wind tunnel clock in order to correlate the pictures to the measured data of the wind tunnel

settings and model configurations. The four still cameras were controlled by a personal computer using the Multi-Camera Control System (software made by Nikon Corp.) in order to simultaneously activate the shutters. The positions of ice were identified with the pre-depicted grids on the model surface and the optically projected grids on ever-shifting ice accretions using a commercially available projector (SX 6000 (Canon Corp.)) with high brightness.

### 3.2 Procedure for Optical Measurement

The procedure of the new method will be described with references to the schematics of the data reduction procedure in [Figure 4a through 4c](#).

(a) Figure 4a: acquire calibration images

Two cameras (or more) are installed so that the target points of ice can be three-dimensionally captured and photographed during the test (for the sake of simplicity, examples of measurement with two cameras are shown). The calibration plate with reference points (shown in the pictures as white circles) is anchored to the model where the angle of attack and the high lift device were set under test conditions in no-wind conditions. The calibration plate is moved around the area where the presence of the runback ice is assumed, which results in a set of the image data of the calibrated reference points being acquired. A three-dimensional space coordinate database as the correlation of the model reference coordinates to the photographic reference coordinates is established on the model.

(b) Figure 4b: acquire images of measurement object and define the target point

Images of the runback ice as the target object for measurement are acquired at an arbitrary time during testing. The positions  $(X_{\text{pix}}, Y_{\text{pix}})_{A, B}$  of the target points in the photographic reference coordinate system of a target point are identified (for the sake of simplicity, the picture shows a simulated runback ice shape for pre-check). After photographing the target object, the target points  $(X_{\text{pix}}, Y_{\text{pix}})_{A, B}$  in the photographic reference coordinate system are set.

(c) Figure 4c: Trace the target points over the calibrated pictures and calculate the positions of the target points

The target points  $(X_{\text{pix}}, Y_{\text{pix}})_{A, B}$  in the photographic reference coordinate system are transferred to the photographic reference coordinates of the calibration plate in no-wind conditions. The values in the model reference coordinate system  $(X_g, Y_g, Z_g)$  of interpolation points  $P_{A1}, P_{A2}, P_{B1}, P_{B2}$  on the calibration plate, are obtained from the correlation of the model reference coordinate system  $(X_g, Y_g, Z_g)$  and the photographic reference coordinate system  $(X_{\text{pix}}, Y_{\text{pix}})$  of the calibration plate. The target point of the ice is obtained as the intersection point of two straight lines  $P_{A1}P_{A2}$  and  $P_{B1}P_{B2}$  on the model reference coordinate system (substantially determine the point as the midpoint of the line with shortest distance between two straight lines since measurement errors exist).

These test procedures for the data reduction of the images enable the provision of information on the height and the position of the intended target point on the runback ice at an arbitrary time.



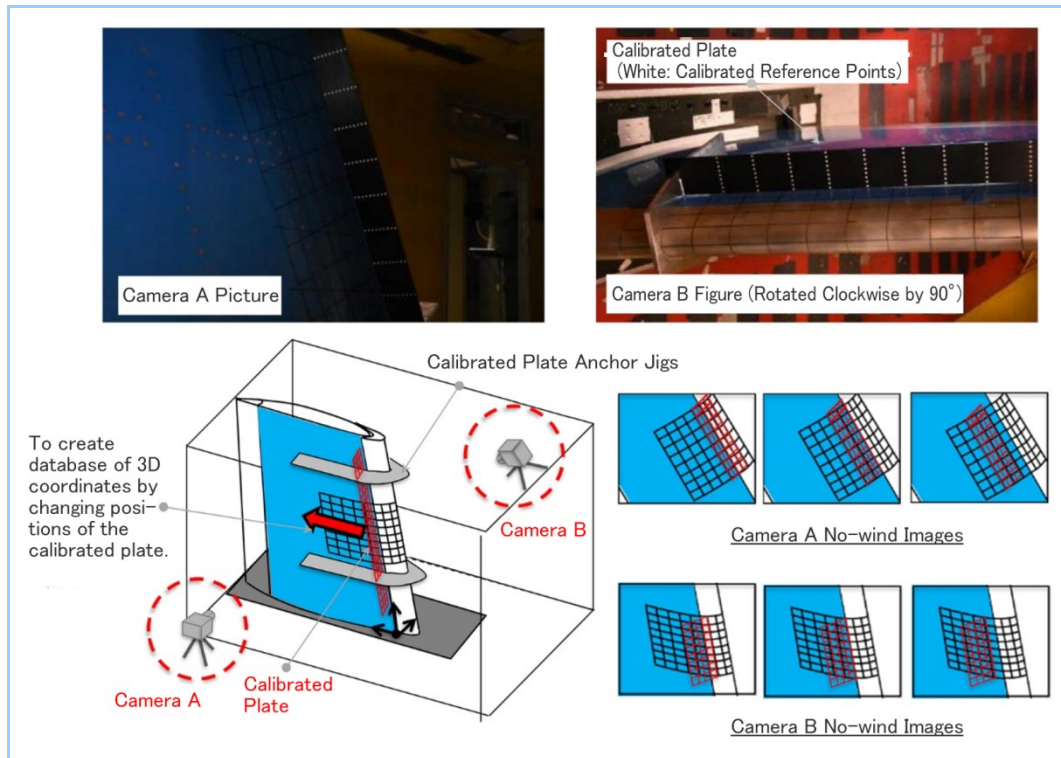


**Figure 4a** Schematic of data reduction procedure—Acquire calibration images

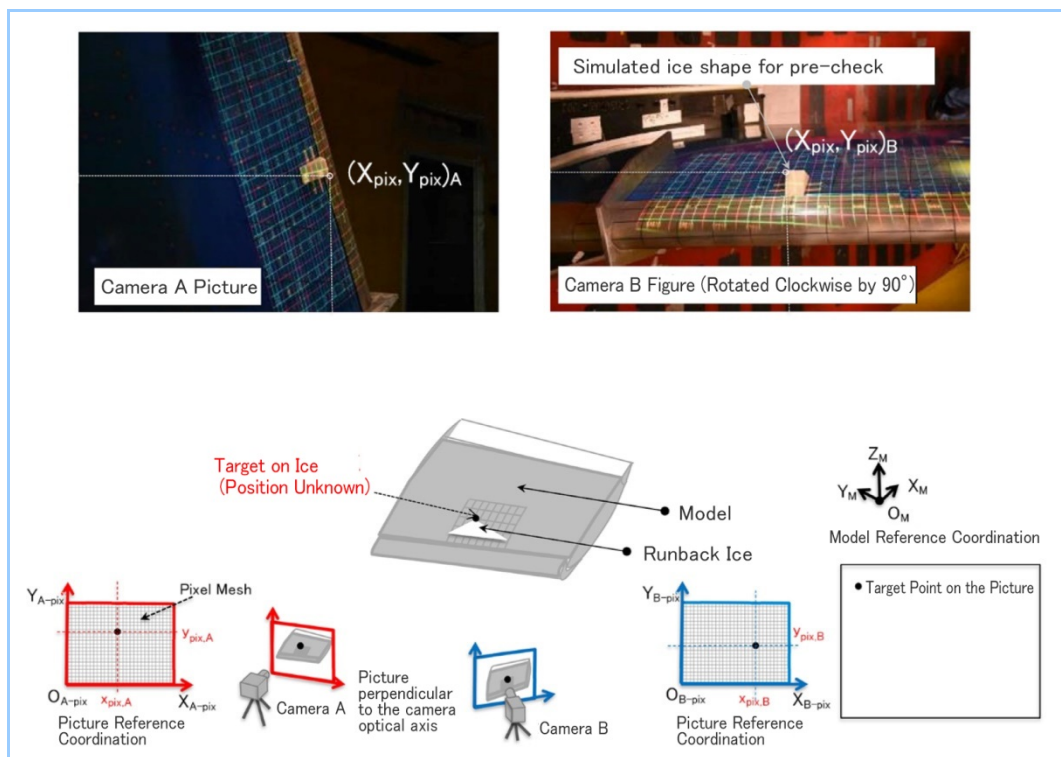


**Figure 4b** Schematic of data reduction procedure—Acquire images of measurement object and define the target point

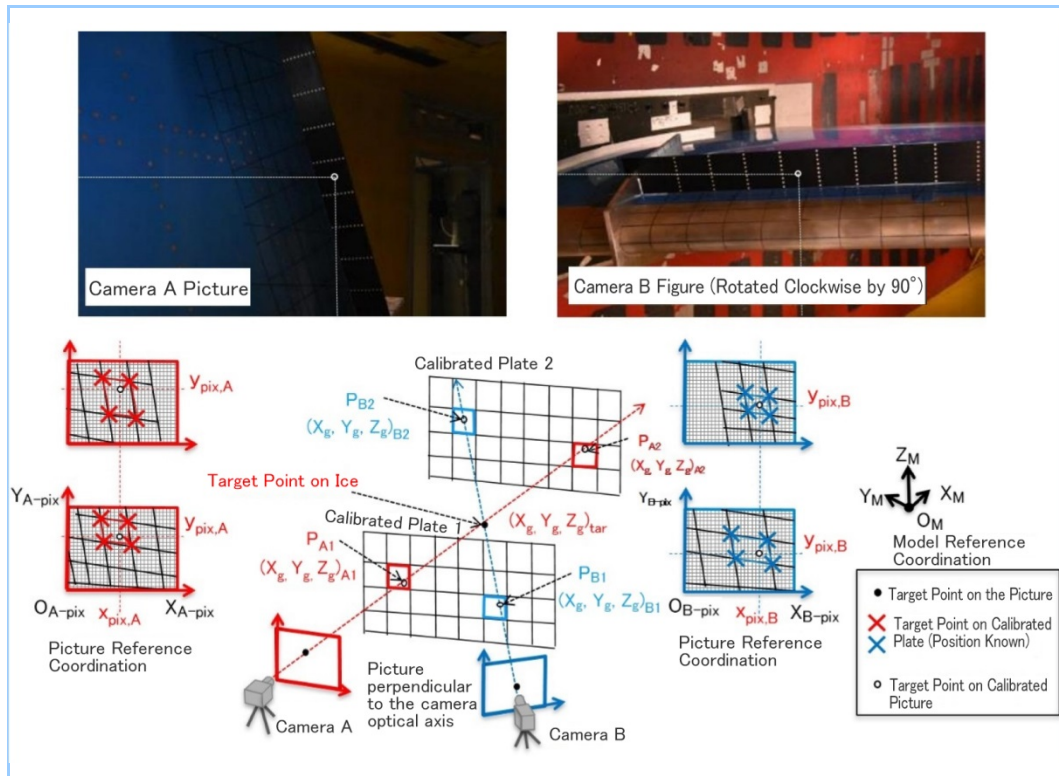


**Figure 4c** Schematic of data reduction procedure—Trace the target point over calibrated pictures and calculate position of target point

### 3.3 Results of optical height measurement and its accuracy verification

**Figure 5** gives examples of the measurement images of the runback ice with fixed time intervals during testing. The outer edge of the accumulated runback ice shape was stereoscopically viewed by the cameras from the front and the rear. Images corresponding to the identical points on a one-to-one basis on the grids projected on the runback ice and the pre-depicted ones in the model, were acquired. Furthermore, images taken from the side were supplementally utilized in order to clarify these correlations.

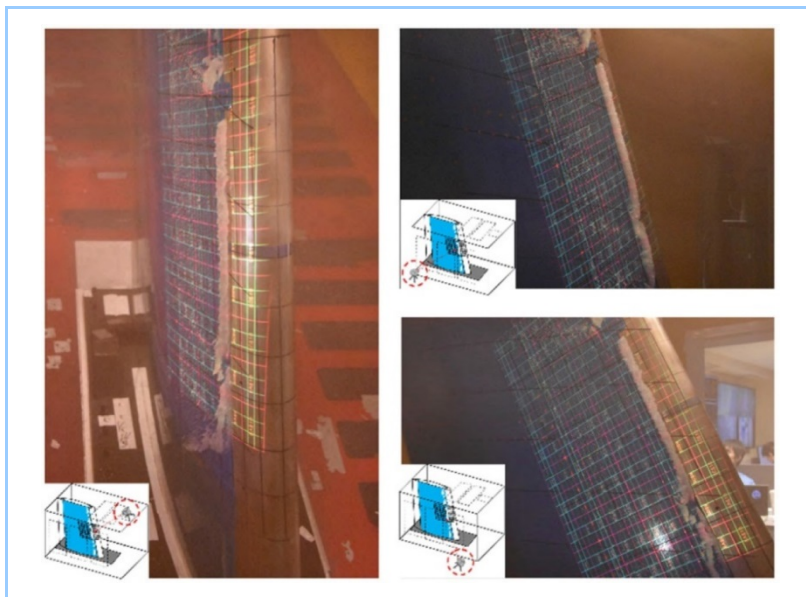


**Figure 5** Examples of optical measurement for runback ice in wind

**Figure 6** shows the results of the optical ice height measurement. From the time series data of Figure 6(a), this method reveals that the phenomenon of the runback ice, which repeats shedding and accumulating processes, was quantitatively evaluated at fixed time intervals. Figure 6 (b) is a height plot of all test data measured. The plot provides the quantitative maximum value of the accumulated ice height under different test conditions for each span region. The acquired data

establishes the appropriate accumulated ice height, position and shape without excessive margin, enabling the prediction of the aircraft performance degradation during flight under icing conditions. These values for flight safety assessment also facilitate the evaluation of the system design, balancing safety, the reduction of environmental impact and the improvement of aircraft fuel efficiency.

Note that the accuracy verification of this optical measurement was carried out after the test by comparing the measurement values with the direct measurement values using a ruler for the runback ice that remained without shedding. **Figure 7** gives the results of the optical measurement accuracy verification. It was confirmed that the measurement accuracy of the height was within  $\pm 0.1$  inches (about 2.5 mm) for direct measurement using a ruler.

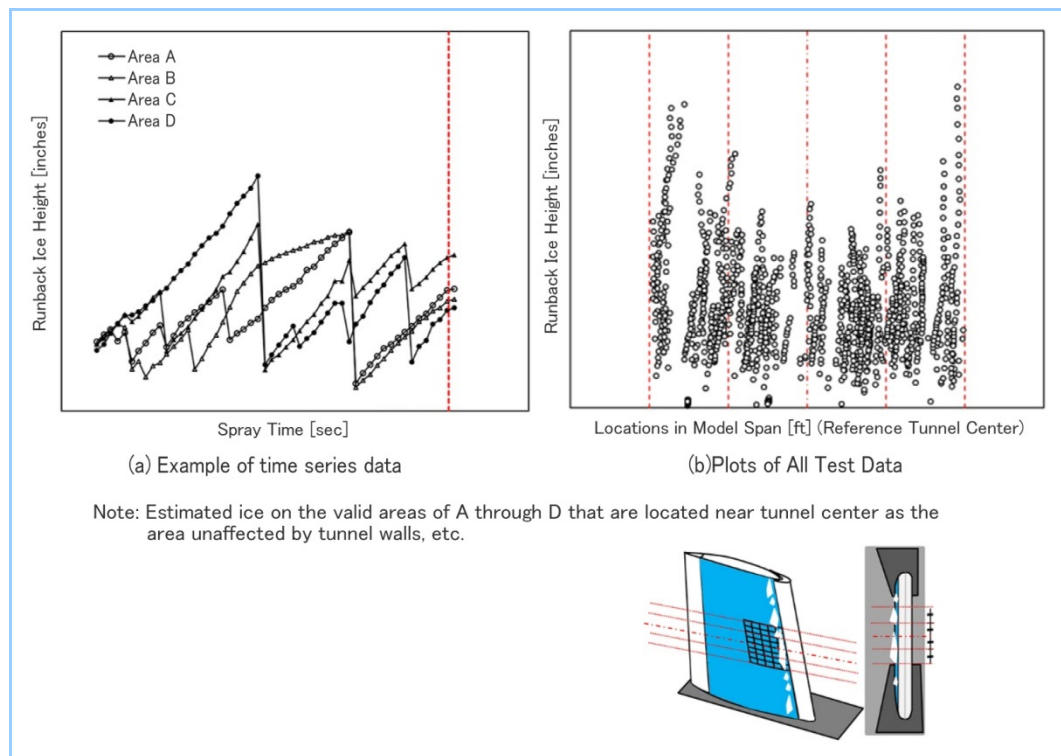


**Figure 6 Results of Optical Ice Height Measurement**

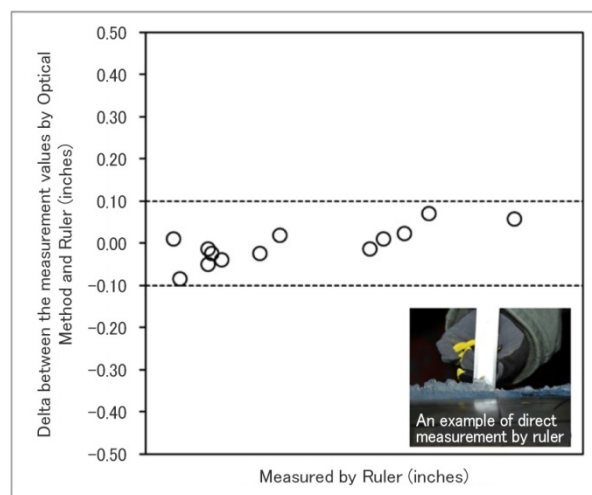


**Figure 7 Accuracy verification of Optical Measurement**

## 4. Conclusions

It is required that the wing anti-ice system of commercial aircraft considering environmental impact and aircraft fuel consumption should be designed while keeping the limitation of engine performance deterioration and the appropriate evaluation for the phenomenon of ice accretion

called runback ice in mind. A new optical measurement technique as a means for proving conformity to aviation regulations has been developed to quantitatively evaluate the time series of runback ice shape, which has the feature of shedding and accumulating.

## References

- (1) A Heinrich et al., Aircraft Icing Handbook Volume 1 of 3, FAA, DOT/FAA/CT-88/8-1, (1991)
- (2) M.B.Bragg et al., Iced-Airfoil Aerodynamics, Progress in Aerospace Sciences, Vol 41, Issue 5, (2005), Pages 323-362
- (3) Airworthiness Standards Part III Aircraft (Airworthiness Classification : Aircraft Transport T)
- (4) 14 CFR Part25 – Airworthiness standards: Transport Category Airplanes
- (5) CS-25 - Certification Specifications for Large Aeroplanes
- (6) AC 20-73A, Aircraft Ice Protection, (2006)
- (7) SAE\_ARD5906, Ice Shape Measurement and Comparison Techniques Workshop, (2003)
- (8) Sam Lee et al, Development of 3-D Ice Accretion Measurement Method, NASA TM, NASA/TM-2012-217702
- (9) R.H.Soeder et al., NASA Glenn Icing Research Tunnel User Manual, NASA TM, NASA/TM-2003-212004
- (10) Saeed, F. et al., Hybrid Airfoil Design Procedure Validation for Full-Scale Ice Accretion Simulation, Journal of Aircraft, Vol. 36, No. 5, 1999, pp.769-776.